 ©2012 Kvantovaya Elektronika and Turpion Ltd

BIOPHOTONICS

PACS numbers: 78.67.Bf; 79.20.Eb; 87.16.dp; 87.80.Dj
DOI: 10.1070/QE2012v042n06ABEH014882

Use of fractional laser microablation and ultrasound to facilitate the delivery of gold nanoparticles into skin *in vivo*

G.S. Terentyuk, E.A. Genina, A.N. Bashkatov, M.V. Ryzhova, N.A. Tsyganova, D.S.Chumakov, B.N. Khlebtsov, A.A. Sazonov, L.E. Dolotov, V.V. Tuchin, N.G. Khlebtsov, O.A. Inozemtseva

Abstract. **The delivery of gold nanoparticles (nanocages coated with a layer of silicon dioxide (40/20 nm)) dispersed in the solution (glycerol + polyethylene glycol-400, 1 : 1) into the skin tissue is studied experimentally *in vivo*. From the data of optical coherence tomography and histochemical analysis it follows that simple application of suspension of nanoparticles is not efficient enough for delivery of the particles into the skin as a result of passive diffusion. It is shown that fractional laser microablation of skin before the application of the suspension, followed by the topical treatment by ultrasound allows penetration through the epidermis layer and delivery of nanoparticles into dermis and hypodermis**

Keywords: *gold nanocages with silicon dioxide coating, delivery of nanoparticles into skin, fractional laser microablation, optical coherence tomography.*

G.S. Terentyuk N.G. Chernyshevsky Saratov State University (National Research University), ul. Astrakhanskaya 83, 410012 Saratov, Russia; Ulyanovsk State University, ul. Tolstogo 42, 432000 Ulyanovsk, Russia; V.I. Razumosky Saratov State Medical University, ul. Bol'shaya Kazach'ya 112, 410012 Saratov, Russia; e-mail: vetklinika@front.ru;
E.A. Genina, A.N. Bashkatov, D.S.Chumakov, L.E. Dolotov, O.A. Inozemtseva N.G. Chernyshevsky Saratov State University (National Research University), Research-Educational Institute of Optics and Biophotonics, ul. Astrakhanskaya 83, 410012 Saratov, Russia; e-mail: eagenina@yandex.ru;
M.V. Ryzhova, N.A. Tsyganova Ulyanovsk State University, ul. Tolstogo 42, 432000 Ulyanovsk, Russia; e-mail: reallady25@mail.ru;
B.N. Khlebtsov Institute of Biochemistry and Physiology of Plants and Microorganisms, Russian Academy of Science, prosp. Entuziastov 13, 410049 Saratov, Russia;
A.A. Sazonov V.I. Razumosky Saratov State Medical University, ul. Bol'shaya Kazach'ya 112, 410012 Saratov, Russia;
V.V. Tuchin N.G. Chernyshevsky Saratov State University (National Research University), ul. Astrakhanskaya 83, 410012 Saratov, Russia; Institute for Problems of Precise Mechanics and Control, Russian Academy of Sciences, Rabochaya ul. 24, 410028 Saratov, Russia; University of Oulu, P.O. Box 4500, FIN-90014, Oulu, Finland; e-mail: tuchinvv@mail.ru
N.G. Khlebtsov N.G. Chernyshevsky Saratov State University (National Research University), ul. Astrakhanskaya 83, 410012 Saratov, Russia; Institute of Biochemistry and Physiology of Plants and Microorganisms, Russian Academy of Science, prosp. Entuziastov 13, 410049 Saratov, Russia;

Received 14 May 2012
Kvantovaya Elektronika **42** (6) 471–477 (2012)
Translated by V.L. Derbov

1. Introduction

The skin provides primary physical and immune protection of the organism from external effects, toxic substances, pathogenic microorganisms, etc. [1] because of different molecular-cellular protection systems, e.g., lysing enzymes, dendrite cells, and macrophages [2, 3]. At the same time the large area and availability to different external actions allow the skin to be used for topical regional and transdermal delivery of therapeutic agents into the blood circulation system [4–6]. In some aspects (low-traumatic character, reduction of side effects, controlled prolongation, etc.) the transdermal method has advantages over the peroral or intravenous administration [6, 7], in spite of the fact that the penetration of hydrophilic substances into the skin through the lipophilic surface layer is hampered [8].

The progress in nanotechnology has led to essential expansion of the field of biomedical applications of nanomaterials [8, 9]. In particular, this field includes dermatology, cosmetology, and the use of nanoparticles as carriers for delivery of drugs [10–12], including delivery into the skin or through it [13]. The development of the latter requires clarifying the mechanisms of interaction between the nanoparticles and the skin, which is a structurally complex biotissue, consisting of epidermis, dermis and hypodermis [14]. Within the epidermis, in turn, five layers are distinguished, namely, the basal, spinous, granular, and translucent layers, and the cornified layer (stratum corneum), which is the main obstacle for nanoparticles to penetrate into the skin [14, 15]. Possible ways of substance migration through the stratum corneum determine three ways of nanoparticle penetration, namely, through the lipid matrix, through the membranes of keratocytes, and through the sebaceous and sudoriferous glands [6], the latter possibly being most efficient [16].

The efficiency of penetration of nanoparticles into skin depends on many factors, which may be also tentatively divided into three groups. The first group consists of the properties of skin itself, including its thickness [17], density of adnexa location [18], degree of stratum corneum hydration [19], blood flow velocity [20], presence of pathology [21], metabolism character [22], etc. The second group includes the size of nanoparticles [23] (and probably their shape), charge [24], surface functionalisation [25], properties of solvent [26] or gel [27], in which the particles are dispersed. The third group of factors includes the external physical and chemical effects, promoting the enhancement of skin permeability for nanoparticles [28]. These effect include ultrasound

treatment [29], horny layers removal using the strip method [30], skin perforation using microneedles [31], photomechanical effect [32], fractional laser microablation [33], ionophoresis [34], ultraviolet irradiation [35], application of chemical permeability enhancers based on solvents of lipid bridges of the stratum corneum [dimethyl sulphoxide (DMSO) and many others] [36, 37], etc.

The wide spectrum of nanoparticles used for topical regional delivery includes liposomes [38], lipid nanostructures [39], polymer nanoparticles [40], nanoparticles based on titanium dioxide and zinc oxide [41], magnetic nanoparticles [42], and also silver [43] and gold [23, 27, 44] nanoparticles. Due to their unique optical properties [45], low toxicity [46] and possibility of funtionalisation with different molecular vectors [47], gold nanoparticles are intensely used in biomedicine [48], including the new area – theranostics, which combines therapeutic and diagnostic facilities in one nanoconstruction [49, 50].

In spite of a variety of gold nanoparticles used at present [9, 48], the number of papers on their capabilities for topical regional and transdermal delivery is extremely limited. Sonavane et al. [23] investigated penetration of gold nanospheres having the diameter 15, 102, and 198 nm into the rat skin *in vitro*. It was shown that the particles with the diameter 15 nm were found both in the epidermal and in the dermal layers of skin, while the penetration of larger particles was minimal. In [44] the penetration of gold nanospheres into the intact and mechanically damaged human skin *in vitro* was compared. Integrally, the damage of the cutaneous covering structure increased the concentration of nanoparticles in the layers of skin. The use of toluene as a disperse medium for the particles of colloid gold having the diameter 15 nm [26] also increased the concentration of nanoparticles in the intact skin, particularly, in the spinous layer of epidermis.

Despite great interest and a variety of publications, the efficient delivery of hydrophilic substances though skin remains an unresolved problem. Trying to solve this problem, the groups of Goto [51] and Niidome [52] proposed to use nanodispersions of the solid-in-oil type on the basis of hydrophobic surface-active substances (SAS). It was shown that such nanoparticles with included insulin have the size ~250 nm and provide the delivery of the preparation into skin almost an order of magnitude faster than the aqueous solution of insulin. In [52] the penetration of the dispersions on the basis of SAS L195, ovalbumin, and m-PEG-coated gold nanorods was studied, and it was shown that the photothermal heating of the latter leads to the enhancement of protein delivery through the skin.

The papers referred above reveal the possibility in principle of topical regional delivery of gold nanoparticles into the skin. However, these data were obtained only in experiments *in vitro*, whereas the properties of intact animal skin are apparently different from those of the samples used in model experiments. Besides, the fact of particular importance is that without supplemental external stimulation the passive delivery of particles into the skin or through it is low-efficient even for small-size nanoparticles (15–20 nm), to say nothing of larger ones. Therefore, it is urgent to improve the efficiency of gold nanoparticles delivery in a wide range of their sizes (from 15 to 200 nm) using different kinds of physical and chemical effects. In particular, it seems promising to use the method of fractional laser microablation in combination with ultrasonic treatment, proposed in [33].

The aim of the present work is to study the possibility of delivering gold nanocages with silicon oxide coating into the tissues of skin *in vivo* using the multimodal approach, including the fractional laser microablation, processing with ultrasound, and special composition for dispersion of nanoparticles.

2. Materials and methods

2.1. Synthesis and characterisation of gold nanoparticles and composition with nanoparticles

To synthesise the gold nanocages the following chemical reagents were used: silver nitrate $AgNO_3$ (more that 99.9%, Aldrich, USA), ethylene glycol (99%, Aldrich, USA), polyvinyl pyrrolidone (M_w = 55000, Sigma-Aldrich, USA), isopropyl alcohol (ChDA, 'Vecton', RF), tetraethyl orthosilicate (98%, Aldrich, USA), 30% aqueous solution of ammonia (Aldrich, USA), acetone (ChDA, 'Vecton', RF), absolute ethanol (99.99%, 64-17-5, Sharlau, Spain), sodium sulphide nonahydrate $Na_2S{\cdot}9H_2O$ (OSCh, GOST 2053-77, RF), liquefied argon (99.99%), deionised water MilliQ (18 MΩ cm, Millipore, USA).

The glass vessels before use were treated with the mixture of nitric and hydrochloric acids ($HCl:HNO_3$ = 3:1) followed by washing with the KOH solution in isopropyl alcohol and, finally, with the deionised water.

The gold nanocages were produced using the two-stage protocol [53]. In short it is the following: 30 mL of ethylene glycol were heated up to 150 °C during 50 min. In the presence of argon flow 0.35 mL of the sodium sulphide solution (0.3 mM) in ethylene glycol, 7.5 mL of the solution of polyvinyl pyrrolidone in ethylene glycol with the concentration 20 mg mL^{-1}, and 2.5 mL of the solution of silver nitrate in ethylene glycol with the concentration 48 mg mL^{-1} were added in sequence. The particles were centrifuged (with the acceleration 10000*g*) during 30 min and resuspended in 40 mL of ethanol. In the magnetic mixer 2 mL of silver cubes were added to 100 mL of the polyvinyl pyrrolidone (1 mg mL^{-1}) and the mixture was heated up to 100 °C. Then 10 mL of tetrachloroauric acid (1 mM) were added in portions of 100 μL each. The colour of the suspension changed from yellow to blue, at the same time the plasmon resonance shifted to 770 nm. The resulting suspension was cooled and 0.7 mL of 30% ammonia was added to it. Then the particles were centrifuged three times (10000*g*) during 30 min each and resuspended in water. In the end of washing the particles were mixed with water to get the optical density 25 at the wavelength 700 nm.

The nanoparticles coated with silicon oxide were produced using the modified Stöber method [54]. 18 mL of isopropyl alcohol were added to 4 mL of suspension of nanocages. In the mixer at room temperature 0.5 mL of ammonia and 25 mL of tetraethyl orthosilicate were added. The duration of the reaction was 50 min. Then the particles were centrifuged five times (5000*g*) during 10 min each and were resuspended in water. In the end of washing the particles were mixed with water up to reaching the optical density 25 at the wavelength 790 nm.

The geometrical parameters of the nanoparticles were found from the transmission electron-microscopic (TEM) images, obtained using the Libra-120 electron microscope (Carl Zeiss, Germany), and their optical properties were con-

trolled by the extinction spectra, measured with the Specord 250 UV-VIS spectrophotometer (Analytic, Jena, Germany). According to the TEM data, the mean size of a gold nanocages was 40 ± 4 nm, the mean thickness of the silicon dioxide layer was 20 ± 3 nm (Fig. 1a), the wavelength of the plasmon resonance before and after coating of nanoparticles with a layer of silicate was 770 and 790 nm, respectively (Fig. 1b).

The preparation of colloid suspension of gold nanocages coated with the layer of silicon dioxide for external use was carried out as follows. A mixture of 95% aqueous solution of glycerol (Close Corporation 'Basa No. 1 khimreaktivov', RF) (refractive index n = 1.467) and polyethylene glycol-400 (PEG-400, M_w = 400, Aldrich, USA) (n = 1.463) in equal parts was prepared. The total volume of the solution was 920 μL (n_s =1.465). The concentrated nanoparticles (1 mL of colloid) were added to the obtained solution drop by drop. Then the entire system was homogenised in the ultrasonic bath (Elmasonic One, Germany) during 10 min. The refractive indices were measured with the IRF-454B2M refractometer (LOMO, Russia) at room temperature (~20 °C) following the standard technique.

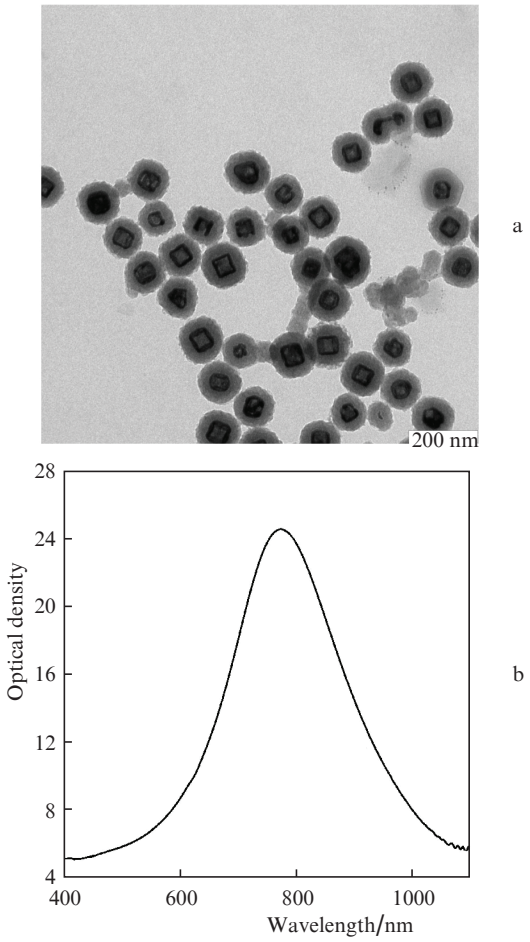

Figure 1. TEM image of gold nanocages coated with silicon oxide (a) and their extinction spectrum (b). The optical density in the spectra is obtained by approximation of the data with the dilution and measurement in the 1-cm-thick cuvette taken into account.

2.2. Experiment

In the study we used male white outbred laboratory rats. In the beginning of the experiment their age was eight weeks and the body mass was ~200 g. The experiment was organised in agreement with the international ethic norms, regulating the experiments in animals in compliance with the Directive 2010/63/EU of the European Parliament and of the Council of 22 September 2010 on the protection of animals used for scientific purposes, European Convention for the Protection of Vertebrate Animals used for Experimental and Other Scientific Purposes (Strasburg, 1986), International rules Good Laboratory Practice for Nonclinical Laboratory Studies of 04.03.2002, and the Order of the Ministry of Health of Russian Federation No. 267 of 19.06.2003 on Authorisation of the Rules of Laboratory Practice. Ten rats were taken for experiments. Directly before the experiment they were subjected to general anaesthesia by intramuscular injection of Zoletil 50 (Vibrac, France).

Before the measurements, the hair was removed from the animals' back by means of the depilatory cream Nair (Church & Dwight Co., Inc. USA) and seven sample area pieces of the hairless skin were selected, each having the dimensions ~2 × 1.5 cm. The suspension containing nanoparticles was topically applied to the experimental area pieces. Two area pieces were used as control ones, one piece of intact skin (Area 1) and the other with applied suspension of nanocages, coated with the layer of silicon dioxide (Area 2). To facilitate the penetration of nanoparticles into skin we used fractional laser microablation (FLMA) and ultrasonic (US) treatment (ultrasonophoresis). Table 1 presents the description of all the seven area pieces of skin.

The suspension of nanoparticles was applied to Area 3 and then it was subjected to ultrasonic treatment. Areas 4–7 were subjected to FLMA directly before the application of the agents under study. This manipulation was implemented by means of the Palomar Lux2940 erbium laser (Palomar

Table 1. Description of control and experimental areas of skin. The suspension base is a mixture of the 95% aqueous solution of glycerol and PEG-400 (1 : 1).

Area number	Series	Methods of skin treatment
1	Control	Intact skin
2		Suspension of nanoparticles coated with a layer of silicon dioxide
3	Ultrasonophoresis (US)	Suspension of nanoparticles coated with silicon dioxide + US
4	Fractional laser microablation	Fractional laser microablation
5		Fractional laser microablation + application of suspension of nanoparticles coated with a layer of silicon dioxide
6	Fractional laser microablation + US	Fractional laser microablation + application of suspension base + US
7		Fractional laser microablation + application of suspension of nanoparticles coated with a layer of silicon dioxide + US

Medical Products, USA) with the following parameters: λ = 2940 nm, triple-peak operation regime with the total energy 3 J, the pulse energy 1 J, and the duration 5 ms. The perforation was implemented by means of a special head creating 169 vertical cone-shaped channels in the 6 × 6 mm^2 area of the skin. The separation between the channels was ~500 μm, the depth of each channel was equal to ~200 μm and the diameter of the channel on the skin surface was equal to ~ 100 μm.

To enhance the skin permeability and to provide a more uniform distribution of nanoparticles in the skin, Areas 1, 6, and 7 were subjected to ultrasonophoresis. The treatment was implemented by means of the Dynatron 125 US transducer (Dynatronics, USA) during 2 min in the continuous-wave regime with the frequency 3 MHz and the power density 1.5 W cm^{-2}. In 30 min after the exposure to ultrasound the surface of the skin was cleaned with a wet tampon to remove the suspension of nanoparticles from the surface.

Optical coherence tomography (OCT) was used for qualitative estimation of accumulation of nanoparticles in the skin under different types of external influence. The imaging was implemented using the optical coherence tomograph Spectral Radar OCT System OCP30SR 022 (Thorlabs Inc., USA) at the wavelength 930 nm. The spectral bandwidth was 100 nm, the output power was 2 mW, the optical depth of scanning was 1.6 mm, and the in-depth resolution of the system was 6.2 μm. The scanning of each area was performed twice, before the beginning of any manipulations and treatment and after the penetration of the studied agents and the removal of their remainders from the surface of the areas under study.

To detect the zones of accumulation of nanoparticles in the skin at topical application we used histochemical staining of the tissue sections with silver nitrate [55]. After removing paraffin the sections of skin were placed for 15 min into 5% solution of silver nitrate in the boiling water bath and then left for 12–24 hours at 40 °C. To remove the silver sediment, the sections were put into 20 % nitric acid. The stained slides were washed with water, dehydrated and cleared with xylene. Comparative morphologic analysis and morphometry of the structures in permanent microslides were carried using the Motic B3 binocular microscope (Motic, China) with the magnification 400× and 600×.

3. Results and discussion

Figure 2 (left) shows the OCT images of the skin areas of the control series (Areas 1, 2, Table 1) and the area, treated with ultrasound after application of suspension of nanoparticles (Area 3, Table 1). In the right part the corresponding averaged profiles of the OCT signal are presented. The averaging was performed over five A-scans in the central part of the tomogram. In the images of intact skin areas (Fig. 2a) with passive application of suspension with the studied nanoparticles (Fig. 2b) and in the areas, subjected to ultrasonic stimulation of nanoparticle penetration (Fig. 2c), the epidermis layer is noticeable. Above the surface of the skin the images of hair are distinguished that give rise to shadow areas in the skin dermis. In the OCT signal profiles the epidermis corresponds to the first peak, the region of dermis, adjacent to the epidermis corresponds to the second peak, and the minimum between these peaks corresponds to the boundary between the epidermis and dermis.

As an estimate of the optical skin probing depth, we used the depth value, corresponding to the signal reduction by the factor of e^{-1}, as compared with the signal level from the

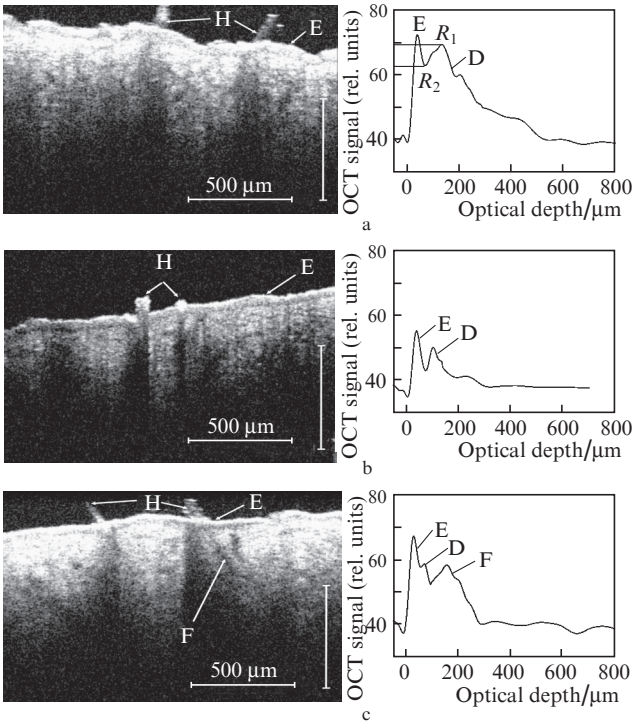

Figure 2. OCT images (left) and profiles of the corresponding OCT signals (right) of the intact skin (Area 1) (a), Area 2 with applied suspension containing nanoparticles (b), and Area 3 treated with ultrasound after applying the suspension (c). The letters label the epidermis (E), dermis (D), hair (H), and follicle (F).

surface of skin. For intact skin this depth amounted to 300–350 μm, for Area 2 it was on the order of 200 μm. The reduction of the optical probing depth may be explained by the shielding effect produced by gold nanoparticles, located on the skin surface and in the hair follicle orifices. This effect is due to both the extra absorption of light by the particles, as compared with the surrounding biotissue [56], and their high reflectance. As a result the OCT signal appears to be significantly lower both from the epidermis and from the dermis tissue. From the analysis of OCT signal profiles in different areas it follows that this reduction amounts to ~1.3 times.

The effect of ultrasound facilitates penetration of nanoparticles suspension into hair follicles. This is confirmed by Fig. 2c, in which a follicle is seen in the depth of the dermis layer. In this case the optical probing depths are practically equal in Area 3 (Fig. 2c) and in the intact skin (Area 1, Fig. 2a). However, after removal of suspension from the surface of skin some nanoparticles stay in the hair follicles, and from Fig. 2c it is seen that the optical depth of probing in Area 3 at the follicle location is significantly smaller (~250 μm) than at the appropriate location of the intact skin (Fig. 2a).

Figure 3 (left) presents the images of Areas 4–7, where FLMA was combined with different effects (see Table 1), and Fig. 3 (right) shows the appropriate averaged profiles of the OCT signal. It is clearly seen that the skin perforation as such does not affect the optical depth of probing, which on average amounted to ~320 μm, close to the value of this parameter in intact skin (see Fig. 2a). The application of nanoparticles suspension onto the skin surface induced significant (on average,

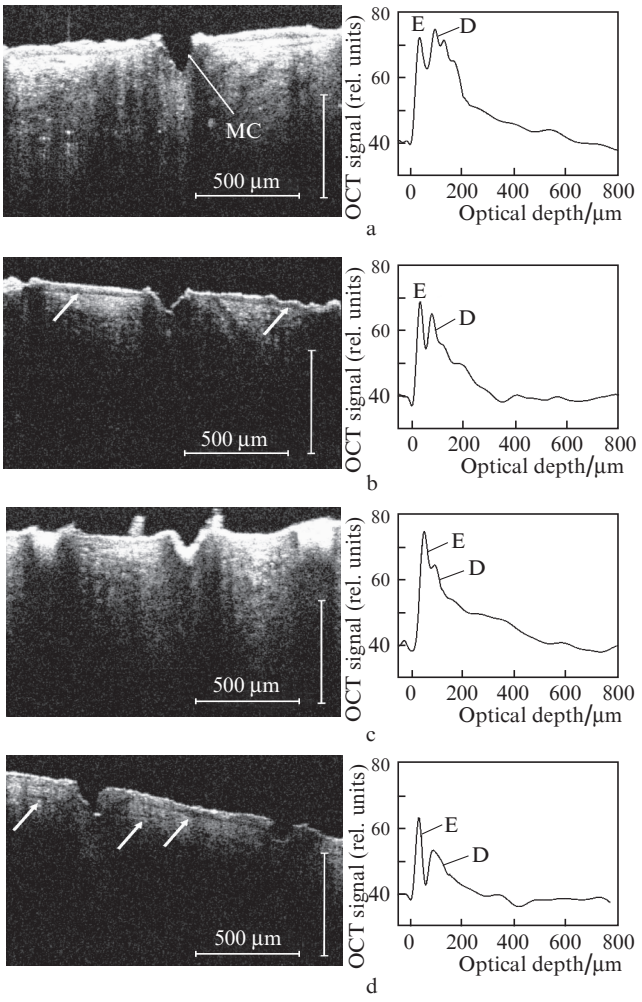

Figure 3. OCT images (left) and profiles of the corresponding OCT signals (right) of the skin areas, subjected to fractional laser microablation: without application of suspension of nanoparticles and US treatment (Area 4) (a), after the application of suspension of nanoparticles (5) (b), after the application of the suspension base and US treatment (6) (c), after application of suspension of nanoparticles and US treatment (7) (d); MC – microchannel.

up to 150 μm) reduction of the optical probing depth in the area between microchannels, and at the very location of microchannels the optical probing depth becomes practically zero (Fig. 3b).

As follows from Fig. 3c, under the combined action of ultrasound and the suspension base, the optical probing depth in the area between the microchannels was equal to ~320 μm, and at the locations below the microchannels it also decreased. Since the mixture of glycerol and PEG-400, serving as the base of the suspension, facilitates optical clearing (reduction of scattering coefficient due to the effect of hyperosmotic immersion agents [57]) of the skin {the refractive index of the solution $n_s = 1.465$ exceeds that of the interstitial liquid $n_{liq} = 1.345$ and is close to that of the basic scatterers in the skin, the hydrated collagen and elastin fibres ($n_c = 1.41 - 1.42$ [58, 59])}, it was expected that the optical probing depth may increase. However, no visible increase in the depth of light penetration into the biotissue was observed. Apparently, this is due to relatively small (~30 min) time of skin exposure to the immersion agent (glycerol and PEG-400) solution, which is, probably, too short for immersing the upper layers of skin. Images of microchannels, filled with the base of the suspension, are clearly seen in Fig. 3c (left) as bright white cone-shaped regions.

Figure 3d illustrates the multimodal effect of FLMA, application of nanoparticle suspension, and ultrasonic treatment on the skin. In this case, in analogy with Area 5, the optical probing depth is reduced, on average, to 120 μm. Apparently, this is due to local compaction of nanoparticles on the skin surface, in the stratum corneum and in near-surface layers of living epidermis in the spaces between the channels, as well as due to the distribution of nanoparticles in dermis in the channels under the action of ultrasound, i.e., as a result of creating a denser reflecting shield, than in the case of passive application of suspension of nanoparticles, that hampers the penetration of probing radiation into deeper layers of skin. At the same time, after the combined action of FLMA, nanoparticles and ultrasound, the structure of skin and its individual layers are clearly seen in the tomogram.

Analysing the images obtained from Areas 2, 3, 5, and 7 (Figs 2b, c and 3b, d), one can notice that the reduction of intensity of the OCT signal, caused by the suspension of nanoparticles, applied to the skin surface or penetrated into the skin depth, favours the increased contrast of imaging of the epidermis and the structure inhomogeneities, located under the skin surface (pointed by arrows in Figs 3b, d, left). The profiles of the OCT signal (Figs 2 and 3, right) allow estimation of the image contrast of epidermis in comparison with the image of dermis as the ratio $(R_1 - R_2)/(R_1 + R_2)$, where R_1 is the OCT signal value from the dermis in the vicinity of the boundary between dermis and epidermis, and R_2 is the OCT signal value from the boundary itself (see Fig. 2a, right). The mean contrast of images for the intact (Fig. 2a) and the perforated (Fig. 3, a) skin amounts to 0.06 ± 0.01, for the skin area with injected base of suspension (Fig. 3c) 0.01 ± 0.004, and for the skin area with injected suspension of nanoparticles (Figs 2b, c and 3b, d) 0.08 ± 0.01 (note that in Fig. 2c the region above a follicle is shown). Thus, as a result of applying the suspension of nanoparticles the mean value of the contrast of the epidermis image increased by 1.3. At the same time the comparison of Figs 3b and d shows that, in spite of coincidence of contrast values at the epidermis–dermis interface, the structure of skin tissue is essentially better visualised in the case, when the ultrasound is applied, in addition to the penetration of nanoparticles and FLMA.

The OCT data on the localisation of nanoparticles on the surface and inside the dermis at different methods of their injection into the skin are confirmed by the data of the histological analysis (Fig. 4). Staining of slides, obtained as a result of biopsy of all skin areas, with silver nitrate allows qualitative estimation of the degree of penetration of nanoparticles into the layers of the cutaneous covering and their localisation. In the case of passive application of the suspension on the skin the character of staining was practically similar to that for the sample of intact skin (Area 1, Fig. 4a). Figure 4b presents a photograph of the histological slide of Area 3, to which the suspension of nanoparticles was applied in combination with the US treatment. A small-size zone of nanoparticle accumulation is seen in the stratum corneum (pointed with arrow). In this case no significant penetration of nanoparticles into the depth of the cutaneous covering occurs. Therefore, the ultrasonophoresis itself does not provide efficient penetration of nanoparticles through the stratum corneum.

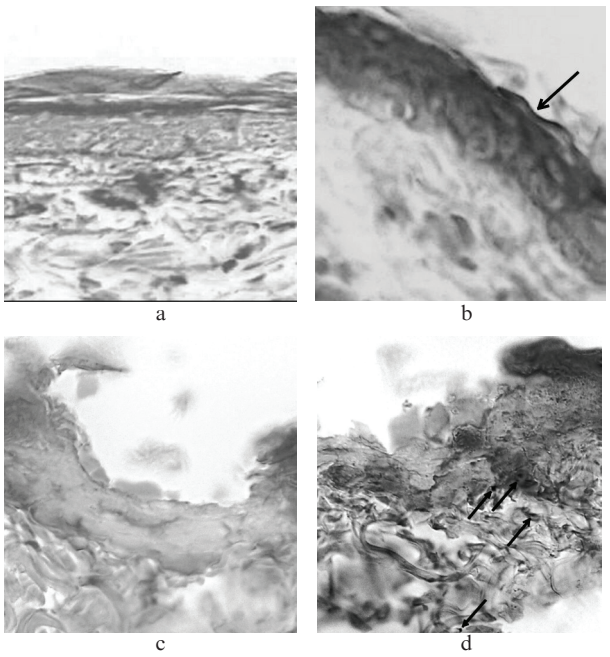

Figure 4. Photographs of histological slides: the intact skin (Area 1) (a); the area after application of suspension of nanoparticles and US treatment (3) (b); after microablation, application of the base of suspension and US treatment (6) (c); and after microablation, application of suspension of nanoparticles and US treatment (7) (d). The images were obtained with the magnification 400× (a) and 600× (b–d). Dark spots correspond to clusters of particles (pointed by arrows).

Figure 4c presents a photograph of a histological slide of Area 6 (see Table 1). The ablation zone surrounded by a layer of coagulated tissue is clearly seen.

In Fig. 4d a zone of ablation is also present; however, in contrast to Fig. 4c, the layer of coagulated tissue in this case is not pronounced. The reason may be the following: under the action of ultrasound the particles begin to move from the surface into the depth, through the layer of coagulation, causing the damage of its integrity. Besides that, in the figure one can clearly see black points, corresponding to nanoparticle clusters stained with silver (pointed by arrows). Extended dark zones indicate uniform distribution of nanoparticles, caused by the additional US treatment on the perforated skin. These zones involve dermis and hypodermis, which confirms the fact that only the combined effect of FLMA and ultrasound leads to accumulation of nanoparticles in deeply located regions of skin tissue.

4. Conclusions

The results of this work demonstrate the possibility in principle of the topical regional delivery of gold nanocages into the deep layers of skin and their deposition under the *in vivo* conditions. However, the mere application of the suspension of nanoparticles to the intact skin is not accompanied by changes in the OCT images and photographs of histological slides, which indicates practical absence of penetration of nanoparticles into the skin via passive diffusion. Therefore, to provide considerable accumulation of nanoparticles of this size in the skin, one has to use physical and chemical agents that enhance the skin permeability.

Fractional laser microablation of epidermis seems to be the most efficient physical method of enhancing the skin permeability among the methods tested by us. The microscopic holes produced as a result of this manipulation allow penetration of nanoparticles into dermis and hypodermis, which is confirmed by the increase in the contrast of OCT images and the visualisation of the zones, where the nanoparticles are accumulated, in the photographs of histological slides.

As such, the ultrasonophoresis does not facilitate essential penetration of gold nanoparticles through the skin barrier. However, its use in combination with the fractional laser microablation is reasonable, since the ultrasonic treatment promotes more uniform distribution of nanoparticles inside the tissue.

Acknowledgements. The work was carried out under the partial support from the Russian Foundation for Basic Research, the Federal Targeted Programme 'Scientific and Scientific-Pedagogical Personnel of Innovative Russia' (State Contract Nos 14.740.11.260, 02.740.11.0484, and 02.740.11.0879), the Foundation of the President of the Russian Federation for the State Support of Young Russian Scientists (Grant No. MK-1057.2011.2), the President of the Russian Federation (Grant for State Support to Leading Scientific Schools of Russian Federation No. NSh-1177.2012.2), the Government of the Russian Federation (Grant for State Support of Research Performed under Supervision of Leading Scientists in Russian Educational Institutions of Higher Professional Education), the European Commission (7th Frame Programme – Photonics4Life, Grant No. 224014), and the Program FiDiPro TEKES (40111/11), Finland.

The authors express their gratitude to Palomar Medical Technologies Inc. (MA, USA) for the offered equipment.

References

1. Lee S.H., Jeong S.K., Ahn S.K. *Yonsei Med. J*., **47**, 293 (2006).
2. Berger C.L., Vasquez J.G., Shofner J., Mariwalla K., Edelson R.L. *Int. J. Biochem. Cell B*, **38**, 1632 (2006).
3. Von Stebut E. *Eur. J. Dermatol*., **17**, 115 (2007).
4. Langer R. *Adv. Drug Deliver. Rev*., **56**, 557 (2004).
5. Prausnitz M.R., Langer R. *Nat. Biotechnol*., **26**, 1261 (2008).
6. Desai P., Patlolla R.R., Singh M. *Mol. Membr. Biol*., **27**, 247 (2010).
7. Hunter R.J., Preedy V.R. (Eds) *Nanomedicine in Health and Disease* (Boca Raton: CRS Press, 2011).
8. Schaefer H., Redelmeier T.E. *Skin Barrier* (Basel, Switzerland: Karger, 1996).
9. Dykman L., Khlebtsov N. *Chem. Soc. Rev*., DOI: 10.1039/c1cs15166e (2012).
10. Farokhzad O.C., Langer R. *ACS Nano*, **3**, 16 (2009).
11. De Villiers M.M., Aramwit P., Kwon G.S. (Eds) *Nanotechnology in Drug Delivery* (New York: Springer, 2009).
12. Duncan B., Kim C., Rotello V.M. *J. Control. Release*, **148**, 122 (2010).
13. Ram B. Gupta, Uday B. Kompella (Eds) *Nanoparticle Technology for Drug Delivery* (New York: Taylor and Francis, 2006).
14. Menon G.K. *Adv. Drug Deliver. Rev*., **54**, s3 (2002).
15. Norlen L. *Int. J. Cosmetic. Sci*., **28**, 397 (2006).
16. Lademann J., Richter H., Teichmann A., Otberg N., Blume-Peytavi U., Luengo J., Weiss B, Schaefer U.F., Lehr C.M., Wepf R., Sterry W. *Eur. J. Pharm. Biopharm*., **66**, 159 (2007).
17. Reed J.T., Ghadially R., Elias P.M. *Arch. Dermatol*., **131**, 1134 (1995).
18. Otberg N., Richter H., Schaefer H., Blume-Peytavi U., Sterry W., Lademann J. *J. Invest. Dermatol*., **122**, 14 (2004).
19. Tagami H. *Int. J. Cosmetic Sci*., **30**, 413 (2008).
20. Clough G., Gush R. *J. Vasc. Res*., **46**, 267 (2009).
21. Lavrijsen A.P., Bowstra J.A., Gooris G.S., Weerheim A., Boddé H.E., Ponec M. *J. Invest. Dermatol*., **105**, 619 (1995).

22. Lockley D.J., Howes D., Williams F.M. *Toxicol. Appl. Pharm.*, **180**, 74 (2002).
23. Sonavane G., Tomoda K., Sano A. Ohshima H., Terada H., Makino K. *Colloid. Surface B*, **65**, 1 (2008).
24. Bolzinger M.-A., Briançon S., Chevalier Y. *Wiley Interdiscip. Rev. Nanomed. Nanobiotechnol.*, **3**, 463 (2011).
25. Ryman-Rasmussen J.P., Riviere J.E., Monteiro-Riviere N.A. *J. Invest. Dermatol.*, **127**, 143 (2007).
26. Labouta H.I., Liu D.C., Lin L.L., Butler M.K., Grice J.E., Raphael A.P., Kraus T., El-Khordagui L.K., Soyer H.P., Roberts M.S., Schneider M. *Pharm. Res.*, **28**, 2931 (2011).
27. Batheja P., Sheihet L., Kohn J., Singer A.J., Micjniak-Kohn B. *J. Contol. Release*, **149**, 159 (2010).
28. Kumar R., Philip A. *Trop. J. Pharmaceut. Res.*, **6**, 633 (2007).
29. Paliwal S., Menon G.K., Mitragotri S. *J. Invest. Dermatol.*, **126**, 1095 (2006).
30. Kuchler S., Abdel-Mottaleb M., Lamprecht A., Radowski M.R., Haag R., Schäfer-Kortinget M. *Int. J. Pharm.*, **377**, 169 (2009).
31. Coulman S.A., Anstey A., Gateley C., Morrissey A., McLoughlin P., Allender C., Birchall J.C. *Int. J. Pharm.*, **366**, 190 (2009).
32. Doukas A.G., Kollias N. *Adv. Drug. Deliver. Rev.*, **56**, 559 (2004).
33. Genina E.A. Dolotov L.E., Bashkatov A.N., Terentyuk G.C., Maslyakova G.N., Zubkina E.A., Tuchin V.V., Yaroslavsky I.V., Altshuler G.B. *Kvantovaya Elektron.*, **41**, 396 (2011) [*Quantum Electron.*, **41**, 396 (2011)].
34. Tomoda K., Terashima H., Suzuki K., Inagi T., Terada H., Makino K. *Colloid Surface B*, **88**, 706 (2011).
35. Mortensen L.J., Oberdorster G., Pentland A.P., Delouise L.A. *Nano Lett.*, **8**, 2779 (2008).
36. Funke A.P., Schiller R., Motzkus H.W., Gunther C., Muller R.H., Lipp R. *Pharmaceut. Res.*, **19**, 661 (2002).
37. Devireddy R.V. *Molecular Reproduction and Development*, **70**, 333 (2005).
38. Elsayed M.M.A., Abdallah O.Y., Naggar V.F., Khalafallah N.M. *Int. J. Pharm.*, **322**, 1 (2007).
39. Uner M., Yener G. *Int. J. Nanomedicine*, **2**, 289 (2007).
40. Guterres S.S., Alves M.P., Pohlmann A.P. *Drug Target Insights*, **2**, 147 (2007).
41. Cross S.E., Innes B., Roberts S.B., Tsuzuki T., Robertson T.A., McCormick P. *Skin Pharmacol. Physiol.*, **20**, 148 (2007).
42. Baroli B., Ennas M.G., Loffredo F., Isola M., Pinna R., López-Quintela M.A. *J. Invest. Dermatol.*, **127**, 1701 (2007).
43. Larese F.F., D'Agostin F., Crosera M., Adami G, Renzi N., Bovenzi M., Maina G. *Toxicology*, **255**, 33 (2009).
44. Filon F.L., Crosera M., Adami G., Bovenzi M., Rossi F., Maina G. *Nanotoxicology*, **5**, 493 (2011).
45. Khlebtsov N.G., Dykman L.A. *J. Quant. Spectrosc. Radiat. Transfer*, **111**, 1 (2010).
46. Khlebtsov N.G., Dykman L.A. *Chem. Soc. Rev.*, **40**, 1647 (2011).
47. Llevot A., Astruc D. *Chem. Soc. Rev.*, **41**, 242 (2012).
48. Dreaden E.C., Alkilany A.M., Huang X., Murphy C.J., El-Sayed M.A. *Chem. Soc. Rev.*, **41**, DOI: 10.1039/c1cs15237h (2012).
49. Chen X. *Theranostics*, **1**, 1 (2011).
50. Khlebtsov B., Panfilova E., Khanadeev V., Bibikova O., Terentyuk G., Ivanov A., Rumyantseva V., Shilov I., Ryabova A., Loshchenov V., Khlebtsov N. *ACS Nano*, **5**, 7077 (2011).
51. Tahara Y., Honda S., Kamiya N., Piao H., Hirata A., Hayakawa E., Fujii T., Goto M. *J. Control. Release*, **131**, 14 (2008).
52. Pissuwan D., Nose K., Kurihara R., Kaneko K., Tahara Y., Kamiya N., Goto M., Katayama Y., Niidome T. *Small*, **7**, 215 (2010).
53. Klebtsov B.N., Khanadeev V.A., Maksimova I.L., Terentyuk G.S., Khlebtsov N.G. *Ross. Nanotekh.*, **5** (7-8), 54 (2010).
54. Ye J., Van de Broek B., De Palma R., Libaers W., Clays K., Van Roy W., Borghs G., Maes G. *Colloids and Surfaces A: Physicochem. Eng. Aspects*, **322**, 225 (2008).
55. Lillie R.D. *Histopathologic Technique and Practical Histochemistry* (New York: McGraw-Hill, 1965).
56. Cang H., Sun T., Li Z-Y., Chen J., Wiley B.J., Xia Y. *Opt. Lett.*, **30** (22), 3048 (2005).
57. Tuchin V.V. *Optical Clearing of Tissues and Blood* (Bellingham, Washington: SPIE Press, 2005).
58. Tuchin V.V. *Tissue Optics: Light Scattering Methods and Instruments for Medical Diagnosis* (Bellingham, Washington: SPIE Press, 2007).
59. Tuchin V.V. *Lazery i volokonnaya optika v biomeditsinskikh issledovaniyakh* (Lasers and Fibre Optics in Biomedical Studies) (Moscow: Fizmatlit, 2010).